UDC 519.61:556.53:532.5
Original scientific paper
Received: 29.12.2012.

Numerical analysis of hysteresis in rating curves for open channel flow

Vanja Travaš, Nino Krvavica and **Ivana Radman**

University of Rijeka, Faculty of Civil Engineering, Radmile Matejčić 3, HR-51000 Rijeka, CROATIA
e-mail: vanja.travas@gradri.hr; nino.krvavica@gradri.hr; ivana.radman@gradri.hr

SUMMARY

For the purpose of studying the hysteresis in rating curves for unsteady flow regime in open channels, a numerical analysis of water wave propagation is performed by a numerical integration of one-dimensional (1D) Saint Venant differential equations. By applying two different boundary conditions, which are specified as the time change in water level h at the upstream boundary of the flow domain, it is shown that the downstream rating curves can obtain the same shapes in the Q-h plane. However, to emphasize the expected difference in rating curves, a third, time axis, is added. Accordingly, the rating curves obtain a spatial shape from which the dynamics of evolution in the relation between the stage h and related discharge Q can be evidenced. Apart from the description of the used numerical formulation (based on the method of characteristics), a numerical example is also presented in the support of the given statements.

***Key words**: rating curve, Saint Venant equations, open channel flow, water wave propagation.*

1. INTRODUCTION

To perform a computational simulation of water wave propagation (which can be related to flood wave propagation), a rating curve, i.e. the functional relation between the water depth (stage) h and volumetric flow rate (discharge) Q, should be specified as a boundary condition at the upstream cross section. However, depending on the length and amplitude of the water wave, two types of rating curves can be recognized. Namely, if the inertial forces associated with local acceleration ($\delta v / \delta t = 0$) can be neglected (if a length of water wave is relatively long and amplitude relatively small) the relationship between the stage h and corresponding discharge Q will be uniquely defined (one-to-one mapping). This scenario can be categorized as a steady flow regime in which the relationship between h and Q can be defined in a purely phenomenological manner by empirical equations (e.g. Manning formula). For such a case, measured stage h can be converted to discharge Q [1, 2].

On the other hand, if a local acceleration is evident ($\delta v / \delta t \neq 0$), the relationship between h and Q will be defined through a closed loop in a Q-h plane [2, 3]. This kind of scenario is closely related to the unsteady behavior of the flow. The closed loop can be interpreted as a hysteresis in a function $Q = f(h)$ i.e. as the fact that under these circumstances the relationship between h and Q depends on the time derivative of h. To reproduce and study this relationship, a numerical model is used herein.

Since the rating curve is defined as a relationship between a stage h and a discharge Q at the same time t, it is obvious that the numerical analysis of hysteresis in rating curve will require a numerical simulation of water wave propagation i.e. a dynamic analysis of unsteady flow. In such a case, for the given upstream boundary condition, the rating curve at the downstream

section can be constructed as a collection of points in a *Q-h* plane defined by stage *h* and discharge *Q* recorded at the same time *t*. Namely, from the practical point of view, it is easy to agree on the fact that the instantaneous measurements of *h* and *Q* in practical consideration are not opportune [4, 5]; therefore, the numerical modeling of such events seems to be adequate for studying their functional relationship.

2. GOVERNING EQUATIONS

The propagations of water waves are a priori unsteady phenomena characterized by temporal variations in water velocity *v* and water depth *h* over the flow domain. To simulate such events, a one-dimensional (1D) flow domain is considered herein. In other words, the components of velocity vector that are perpendicular to the direction of the flow are neglected. The governing equations are particularly introduced for a rectangular cross section of an open channel with constant bed slope S_0. In this case, the cross section area *A* is linearly dependent on a water level *h* and is defined as a product of the water level *h* and the width *B* of the channel. Since the unknown variables are *v* and *h*, the analysis requires a set of two differential equations.

By assuming that there are no lateral inflows, the first governing equation can be written as:

$$\frac{\partial h}{\partial t}+\frac{A}{B}\frac{\partial v}{\partial t}+v\frac{\partial h}{\partial x}=0 \qquad (1)$$

which represents the differential form of a mass conservations for a non-compressible fluid. To form a system of equations, apart from the mass balance Eq. (1), the conservation of linear momentum is applied. By considering only the gravity force, pressure gradient and friction force, the resulting equation is defined as:

$$\frac{\partial v}{\partial t}+v\frac{\partial v}{\partial x}+g\frac{\partial h}{\partial x}=g\left(S_0-S_E\right) \qquad (2)$$

in which S_E represent the slope of energy gradient line and *g* is acceleration of gravity field. Equations (1) and (2) are known as Saint Venant equations. To specify the interaction between the water and the channel, a constitutive equation should be defined for S_E. For this purpose, i.e. to quantify the slope of energy gradient line, a Manning equation is used:

$$S_E=\left(\frac{nQ}{AR^{\frac{2}{3}}}\right)^2 \qquad (3)$$

in which *n* denotes the Manning roughness coefficient [6]. For a given boundary and initial conditions, the system of equations specifies a unique solution in terms of $v(x,t)$ and $h(x,t)$.

3. NUMERICAL FORMULATION

Before performing a numerical discretization of a system defined by Eqs. (1) and (2), it is opportune to apply the method of characteristics to transform the system of partial differential equations into a set of ordinary differential equations [7]. The process is valid for a system of hyperbolic partial differential equations of the first order. Briefly, the essence of this method is to introduce a restriction which will specify a solution of the system over predefined characteristics which can be geometrically interpreted as lines in two dimensional *x-t* solution plane. By applying the method of characteristics, the system defined by Eqs. (1) and (2) obtains the form:

$$\frac{Dv}{Dt}\pm\frac{g}{c}\frac{Dh}{Dt}=g\left(S_0-S_E\right)\quad on:\frac{dx}{dt}=v\pm c \qquad (4)$$

in which *c* denotes the wave celerity and $D\bullet/Dt$ the material-time derivative [8]. Equation (4) defines two equations that are known as positive characteristic and negative characteristic [7]. To further simplify the numerical description, there are a few common assumptions that can be made. According to the real physical behaviour, it is assumed that the surface tension can be neglected. In this case, and by assuming a small wave amplitude, the celerity *c* can be approximated with the linear Airy wave theory as:

$$c=\sqrt{\frac{g\lambda}{2\pi}tanh\frac{2\pi h}{\lambda}} \qquad (5)$$

in which λ denotes the water wave wavelength. Furthermore, by considering that the wave wavelength λ is much greater than the water depth *h*, Eq. (5) can be reduced to $c=\sqrt{gh}$ [7]. It follows that the previous equations defines the relationship $h=c^2/g$. After operating with the material-time derivative on both sides of this equation, it follows that $Dh / Dc = 2c / g$. This equality can be used to simplify Eq. (4) which can be done by rearranging the expression in the following form $Dh = (2g / c)\, Dc$. Accordingly, Eq. (4) can be rewritten as:

$$\frac{D\left(v\pm 2c\right)}{Dt}=g\left(S_0-S_E\right)\ on:\frac{dx}{dt}=v\pm c \qquad (6)$$

To obtain a numerical approximation of Eq. (6), the continuous spatial and temporal domains are discretized by a finite number of points in which the solution of the governing Eq. (6) is approximated. The spatial domain, which is defined between the coordinate *0* and length of the channel *L* is discretized by a finite number of $n\Delta x$ computational cells. Between two neighboring computational cells, the increment Δx is assumed to be constant. The temporal domain is also equidistantly discretized by a finite number $n\Delta t$ of time steps (the time increment Δt is also assumed to be constant). After defining the spatial and temporal discretizations, the numerical approximation of derivatives in Eq. (6)

is computed by the forward Euler method [9]. For this purpose the subscript i is introduced to indicate the spatial position of any relevant physical quantity and the superscript n is introduced to denote the temporal position of the same quantity. Accordingly, the time derivatives can be approximated so that the discrete form of the positive characteristic C^+ becomes:

$$\frac{(v+2c)_i^{n+1}}{\Delta t} - \frac{(v+2c)_{i-1}^{n}}{\Delta t} = g\left(S_0 - S_E\right)_{i-1}^{n} \quad (7)$$

and the negative characteristic denoted by C^- can be analogically rewritten as:

$$\frac{(v-2c)_i^{n+1}}{\Delta t} - \frac{(v-2c)_{i+1}^{n}}{\Delta t} = g\left(S_0 - S_E\right)_{i+1}^{n} \quad (8)$$

The unknown values v^{n+1} and c^{n+1} in the time position $n+1$ and in every computational cell i between the boundary conditions can now be explicitly expressed and calculated from the known initial and boundary conditions [10]. However, since the numerical integration is explicit, it is necessary to satisfy the criteria for numerical stability [11].

3.1 Initial conditions

The initial conditions are given as a velocity $v(x) = v_0$ and depth $h(x) = h_n$ along the flow domain ($0 \le x \le L$) and at the beginning of the computational process. Since the considered channel is prismatic i.e. it is characterized by a constant bed slope S_0, cross section A and roughness n, the initial conditions are here defined with the normal depth $h_n = const.$ [8], calculated for a given initial discharge Q_0.

3.2 Upstream boundary condition

The specification of boundary condition at the inflow i.e. at the upstream section depends on the value of Froude number Fr [6]. In both cases the boundary conditions are specified as functions of time. In particular, for $Fr < 1$, from the given function $h(t)$ at the upstream boundary a related discharge $Q(t)$ can be computed from the negative characteristic [8]. On the other hand, if $Fr > 1$; both water depth $h(t)$ and discharge $Q(t)$ should be specified at the computational cell on the section of the upstream boundary. It should be noted that the rating curve defined only in a Q-h plane is evidently not sufficient since the temporal evolutions of both quantities are needed. This will be shown by considering two different flow scenarios that result in the same rating curve (in a Q-h) plane at the downstream boundary.

3.3 Downstream boundary condition

At the last computational node a so called zero gradient boundary condition is defined for both velocity v and water level h (i.e. celerity c). From the physical point of view this kind of boundary condition will describe a free boundary condition i.e. a boundary condition without solid obstacle. At the numerical implementation level, this boundary condition is simply defined by specifying that $q_{n\Delta x} = q\, n_{\Delta x-1}$ where q can be any relevant quantity.

4. NUMERICAL ANALYSIS

To investigate the hysteresis in rating curves for unsteady flow regime in prismatic open channels, two sets of numerical experiments were carried out for different upstream boundary conditions. Previously described numerical algorithm was used and implemented in a program code written in MathCAD15 [12]. The aim of these numerical experiments is to obtain similar rating curves in a Q-h plane with very distinct stage and discharge hydrographs, as an example of dynamic differences between rating curves evolutions.

A hypothetical case of water wave propagation in a river channel was analyzed. The length of the channel is *7.0 km*, with constant bed slope of S_0=*0.01%* and uniform Manning's roughness coefficient n=*0.015 s/m$^{1/3}$*, which has a prismatic cross section *8.0 m* wide. Initial conditions were defined by calculated normal water depth h_n=*1.06 m* for the initial discharge of Q_0=*5 m^3/s*. The shape of the upstream flood wave (stage hydrograph) was described using the expression:

$$h(t) = \Delta h \left| max\left(\frac{t_p - t}{t_p}, 0\right) - 1 \right|^{ch} \exp\left(\frac{max\left(t - t_p, 0\right)}{cs}\right) + h_n \quad (9)$$

where $h(t)$ is water level at a time t, Δh is maximum water elevation, t_p is time of the flood wave peak, h_n is normal water level, and ch and cs are function shape parameters of the rising and falling segment of the flood wave, respectively.

Two different flood waves were considered (a medium steep flood wave and a fast rising one). The following cases are defined as flows:

* **Case No.1:** considered a propagation of a medium steep flood wave with shape parameters ch=*2.2* and cs=*550*, and with a water level rise of Δh=*1.2 m* occurring at the time t_p=*3600 s*.
* **Case No.2:** considered a propagation of a fast rising flood wave with shape parameters ch=*1* and cs=*500*, and with a water level rise of Δh=*1,2 m* occurring at the time t_p=*2000 s*.

These waves were introduced into the numerical model as the unsteady upstream boundary conditions in a form of a stage hydrograph (Figure 1). The total simulation time was *9000 s* (*2.5 hours*). The temporal discretization was defined by a time step Δt equal to *3.67 s* and the spatial discretization was defined with a space increment Δx equal to *28 m*.

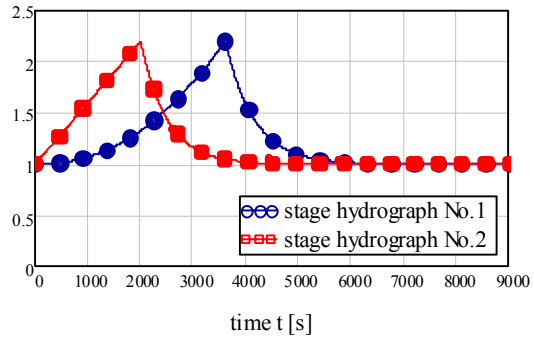

Fig. 1 Upstream stage hydrographs for cases No.1 and No.2

Visualization of the flood wave propagation through the channel is presented in Figure 2 for the second numerical experiment (case No. 2) and for a segment of time from t_1=*2000 s* to t_2=*3000 s*. The following six pictures represent a 3D perspective view of instantaneous water surface along the channel (in a distorted scale).

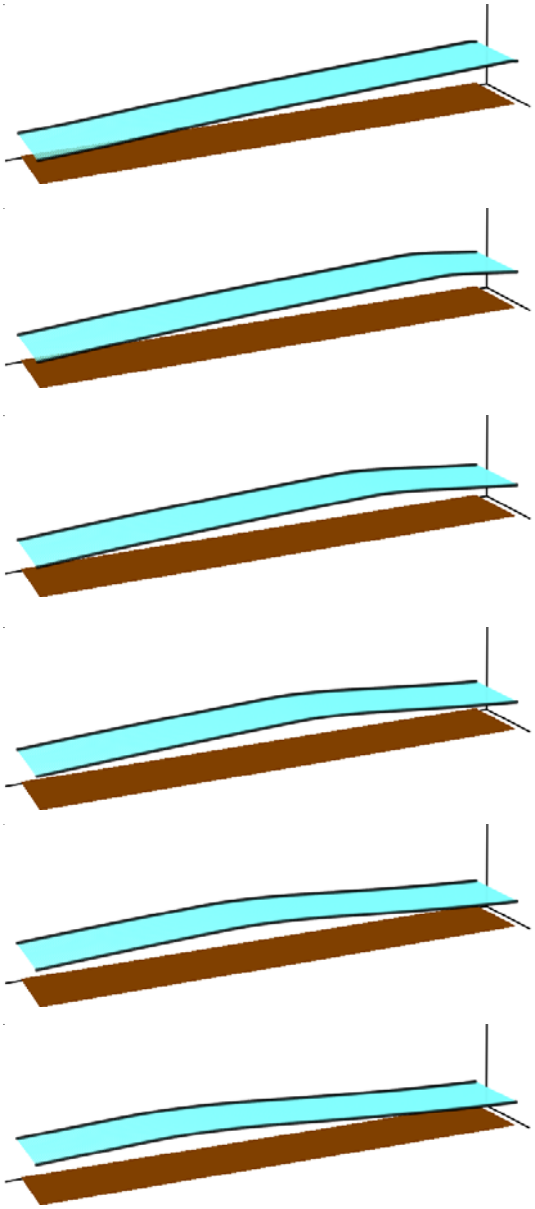

Fig. 2 Visualization of instantaneous water surface for case No. 2, six time steps from t_1=2000 s to t_2=3000 s

Figures 3 and 4 show the results of the numerical experiments (cases No. 1 and No 2, respectively) in terms of upstream and downstream stage hydrographs i.e. hydrograph transformation. It is interesting to notice that the time period elapsed between the occurrence of the downstream stage hydrograph peak and its corresponding upstream peak is almost the same in both cases.

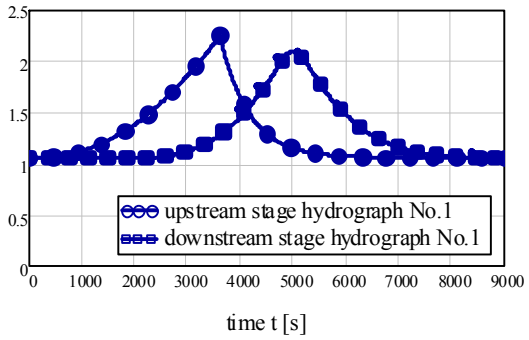

Fig. 3 Upstream and downstream stage hydrographs for case No. 1

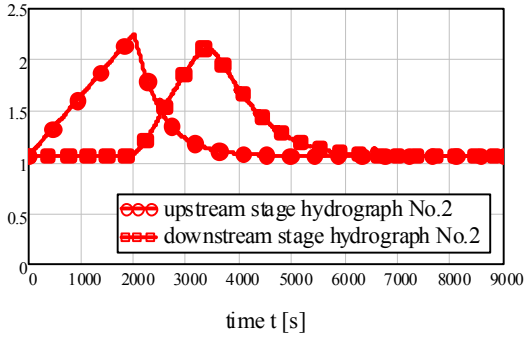

Fig. 4 Upstream and downstream stage hydrographs for case No. 2

It is also interesting to note that, although the shape of the upstream hydrograph No. 1 is very different in comparison with the hydrograph No. 2 (Figure 1), the maximum water levels are almost the same in both cases (h_{1max}=*2.10 m* and h_{2max}=*2.11 m*), as are the shapes of the falling sides of hydrographs, except that they appear at different time steps (Figure 5).

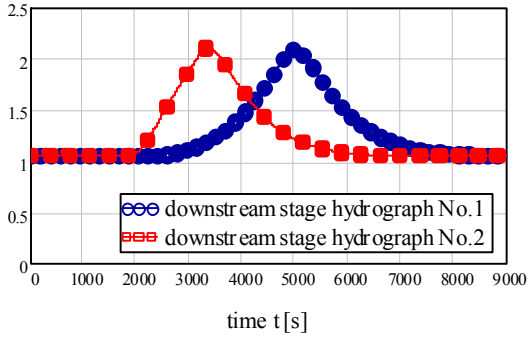

Fig. 5 Downstream stage hydrographs for cases No. 1 and No. 2

Figures 6 and 7 show the rating curves for steady and unsteady hydraulic flow regime with marks for equidistant time positions (cases No. 1 and No. 2, respectively). As expected, for a positive time derivative of *h*, the rating curve for the unsteady flow is below the rating curve for the steady flow and vice versa. It is noticeable that the rating curves for the unsteady flow are very similar, except for a small segment of the curve below the rating curve for the steady flow. On the other hand, time steps differ noticeably, especially in the region below the rating curve for the steady flow, which is to be expected because the upstream stage hydrographs for cases No. 1 and No. 2 differ mostly during the period of flood wave rising.

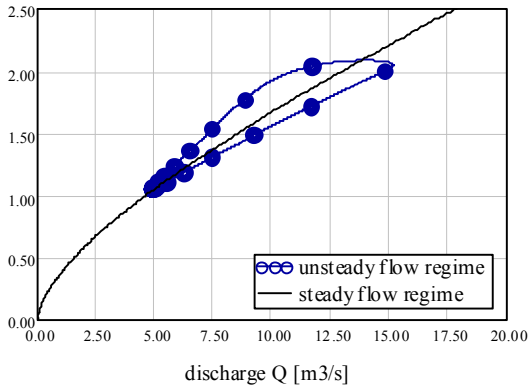

Fig. 6 Rating curves for steady and unsteady flow regime, for case No. 1

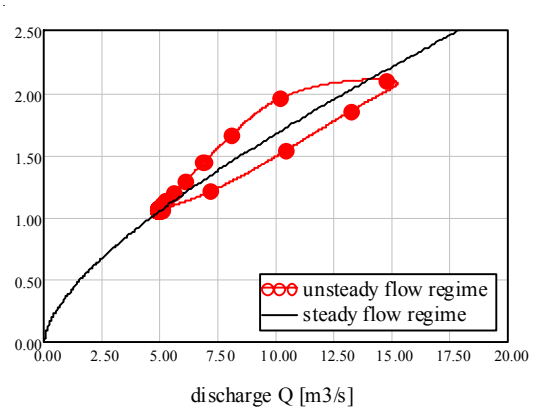

Fig. 7 Rating curves for steady and unsteady flow regime, for case No. 2

Results are also presented in a spatial 3D plot (Figure 8) which shows temporal evolution of rating curves together with the corresponding plane projections: discharge hydrograph on the left, stage hydrograph on the right and rating curve on the bottom plane.

At this point it is important to emphasize that, although the rating curves are almost identical in a *Q-h* plane (Figure 8), time development of the rating curve differs significantly, as do discharge and stage hydrographs.

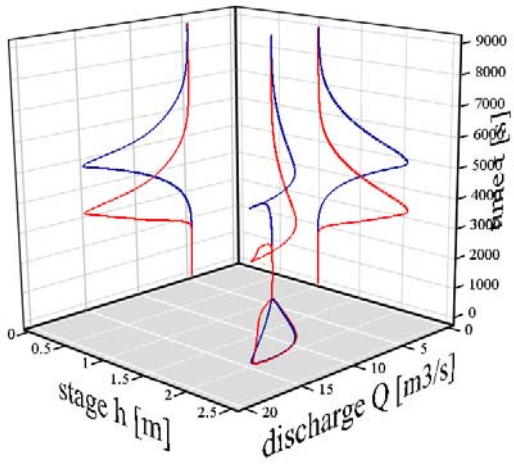

Fig. 8 3D temporal evolution of rating curves for cases No. 1 and No. 2 with corresponding plane projections

5. CONCLUSIONS

Based on the numerical analysis performed by numerical integration of the Saint Venant equations, dynamic characteristics of rating curves have been shown, with emphasis on their temporal evolution. To evidence such processes, rating curves should be presented in a three-dimensional (3D) space or at least in a *Q-h* plane (as they commonly are), but with equidistant time marks. Namely, as illustrated by Figs. 6 and 7, for two different water waves (boundary conditions), almost the same rating curve in a *Q-h* plane is evidenced. In other words, contradictory to the instantaneous measurements of *h* and *Q* in some real flow environment (e.g. rivers), a numerical simulation of water wave propagation can be used in studying the relationship between *h* and *Q* in unsteady flow conditions. However, it should be noted as well that it will be far easier to consider the same physical event reproduced in a laboratory environment than in the real environment conditions. Consequently, in order to investigate further the time evolution of rating curves in unsteady flow conditions, some future work should be done in this direction [13].

6. REFERENCES

[1] G. Di Baldassarre and P. Claps, A hydraulic study on the applicability of flood rating curves, *Hydrology Research*, Vol. 42, No. 1, pp. 10-19, 2011.

[2] F. Dottori, M.L.V. Martina and E. Todini, A dynamic rating curve approach to indirect discharge measurement, *Hydrology and Earth System Sciences*, Vol. 13, No. 6, pp. 847–863, 2009.

[3] M. Delphi, Application of characteristics method for flood routing (Case study: Karun River), *Journal of Geology and Mining Research*, Vol. 4, No. 1, pp. 8-12, 2012.
[4] J.D. Fenton, Rating curves: Part 1 – Correction for surface slope, Proc. 6th Conference on Hydraulics in Civil Engineering: The State of Hydraulics, Hobart, 2001., Ed. A.C.T. Barton, pp. 309-317, 2001.
[5] A. Domeneghetti, A. Castellarin and A. Brath, Assessing rating-curve uncertainty and its effects on hydraulic model calibration, *Hydrology and Earth System Sciences*, Vol. 16, No. 4, pp. 1191–1202, 2012.
[6] M. Mohan Das, *Open Channel Flow*, Prentice-Hall of India Private Limited, New Delhi, 2008.
[7] A.J. Crossley, Accurate and efficient numerical solution for Saint Venant equations of open channel flow, PhD Thesis, University of Nottingham, 1999.
[8] K. Subramanya, *Flow in Open Channels*, Tata McGraw-Hill Publishing Company Ltd., 1997.
[9] E. Kreyszig, *Advanced Engineering Mathematics*, 9th edition, John Wiley & Sons Inc., 2006.
[10] G. Akbari and B. Firoozi, Implicit and explicit numerical solution of Saint Venant equations for simulating flood wave in natural rivers, Proc. 5th National Congress on Civil Engineering, Mashhad, 2010., Ferdowsi University of Mashhad, 2010.
[11] J. Huang and C.C.S. Song, Stability of dynamic flood routing schemes, *ASCE Journal of Hydraulic Engineering*, Vol. 111, No. 12, pp. 1497-1505, 1985.
[12] MathCAD15, PTC Product & Service Advantage, www.ptc.com/product/mathcad/
[13] K. Ashida and T. Takahashi, On the characteristics of flood waves under various boundary conditions, *Bulletin of the Disaster Prevention Research Institute of the Kyoto University*, Vol. 16, Part 3, No. 115, 1967.

NUMERIČKA ANALIZA HISTEREZE KONSUMPCIJSKE KRIVULJE ZA STRUJANJE U OTVORENIM KORITIMA

SAŽETAK

U svrhu analize histereze konsumpcijske krivulje za nestacionarno strujanje u otvorenim koritima, provedena je numerička integracija sustava Saint Venant-ovih jednadžbi te simulacija propagacije vodnog vala. Definirajući dva različita rubna uvjeta na uzvodnoj granici otvorenog korita, koji su specificirani putem vremenske promjene razine vode h na istom profilu, pokazalo se da konsumpcijska krivulja na nizvodnom profilu može poprimiti isti oblik u Q-h ravnini. Pritom, kako bi se pokazalo da su dobivene konsumpcijske krivulje različite, dodala se treća koordinatna os tj. os vremena unutar kojeg vodni val prolazi kroz nizvodni profil korita. Sukladno navedenom, konsumpcijske krivulje su prikazane kao prostorne krivulje s evidentnim razlikama. Osim kratkog pregleda korištene numeričke formulacije (bazirane na metodi karakteristika), prikazan je i numerički primjer unutar kojeg je vidljiva razlika u prostornim konsumpcijskom krivuljama koje dijele zajedničku projekciju u Q-h ravnini.

Ključne riječi: *konsumpcijska krivulja, Saint Venant-ove jednadžbe, strujanje u otvorenim koritima, transformacija vodnog vala.*